



Supplement of

Evaluation of total ozone measurements from Geostationary Environmental Monitoring Spectrometer (GEMS)

Kanghyun Baek et al.

Correspondence to: Jae Hwan Kim (jaekim@pusan.ac.kr)

The copyright of individual parts of the supplement might differ from the article licence.

10 S1. Generation of look-up tables for total ozone column retrieval

The VLIDORT version 2.6 radiative transfer (RT) model (Spurr, 2008) is used to generate radiance look-up tables (LUTs) for the GEMS total column ozone algorithm, using ozone profile climatology and nominal global average temperature profile from the TOMS standard profile climatology (Bhartia and Wellemeyer, 2002, Wellemeyer et al. (1997). Figure S1 shows the eleven ozone profiles and a single temperature profile used in creating the LUTs for the algorithm.

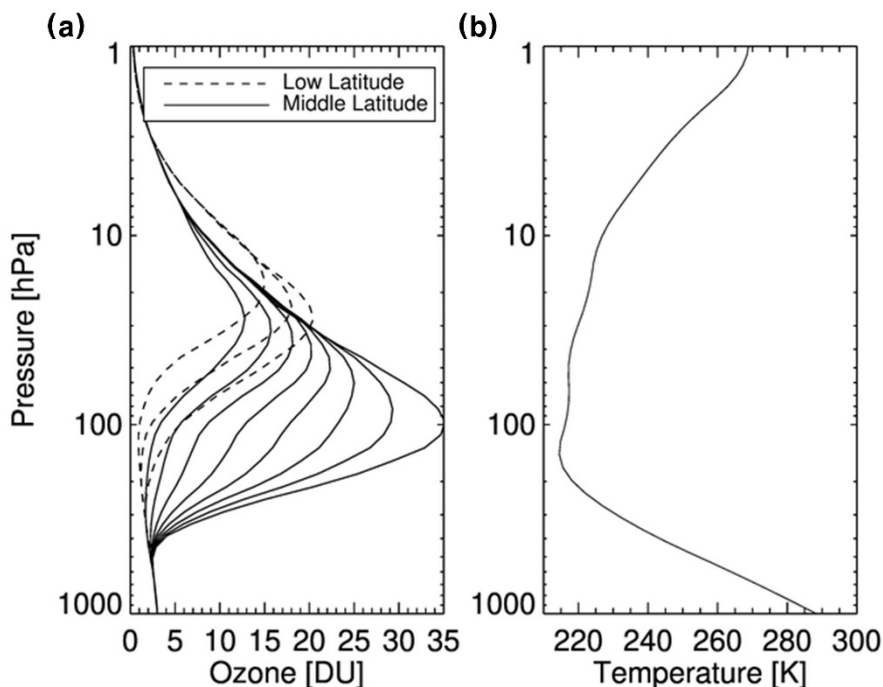


Figure S1. (a) TOMS standard ozone profiles and (b) US standard temperature profile for look-up table generation. The shape of the TOMS standard ozone profiles depends on the total ozone amount and is binned in steps of 50 DU. For the GEMS total ozone retrieval, we use three profiles with 225–325 DU at low latitudes (EQ – 30°N) and eight profiles ranging from 225–575 DU at mid-latitudes (30°N – 60°N).

As mentioned in the manuscript, the BDM ozone cross-section data (Daumont et al., 1992; Brion et al., 1993; Malicet et al., 1995) is used to generate the LUTs. The high-resolution dataset is convolved with GEMS slit functions which have a full width at half maximum (FWHM) of approximately 0.6 nm, and interpolated to seven wavelengths (312.34, 317.35, 331.06, 340, 354, 360 and 380 nm). The top-of atmosphere radiance I_c is divided into a pure atmospheric scattering radiance I_a ($R_s=0$) term and a surface-reflected radiance term I_s .

$$I_c = I_a + I_s \quad (S1a)$$

$$I_a = I_0(\theta_0, \theta) + I_1(\theta_0, \theta)\cos\phi + I_2(\theta_0, \theta)\cos2\phi \quad (S1b)$$

$$I_s = \frac{R_s T}{1 - R_s S_b} \quad (S1c)$$

30

I_a represents the purely atmospheric contribution to the radiance with a black surface bounding a Rayleigh atmosphere. I_a is expressed as a Fourier expansion in the cosine of the relative azimuth angle (ϕ). T and S_b account for atmospheric directional transmissivity and the spherical albedo of the atmosphere, respectively. I_1 and I_2 are converted into Z_1 and Z_2 as follows:

35

$$\begin{aligned} Z_1(\theta_0, \theta) &= \frac{1}{k_1} \frac{I_1(\theta_0, \theta)}{I_0(\theta_0, \theta)}, \\ Z_2(\theta_0, \theta) &= \frac{1}{k_2} \frac{I_2(\theta_0, \theta)}{I_0(\theta_0, \theta)}, \end{aligned} \quad (S2a)$$

where

$$k_1 = -\frac{3}{8} \cos\theta_0 \sin\theta_0 \sin\theta; \quad k_2 = \frac{3}{32} \frac{(\sin\theta_0 \sin\theta)^2}{\cos\theta}. \quad (S2b)$$

40

Z_1 and Z_2 are smooth and well-behaved (non-singular) functions of θ_0 and θ . I_0 , Z_1 , Z_2 , T , and S_b are stored in LUTs as a function of wavelength, total column ozone, surface pressure, solar zenith angle, and viewing zenith angle. The overall nodes of the LUTs are specified in Table S1, and the dimensions of the separate LUTs variables are presented in Table S2.

45

Table S1. LUT parameters and their specification. Note that the relative azimuth dependence is considered explicitly through the Fourier coefficients of path radiance, and the surface albedo dependence is taken into account by the planetary problem.

Parameter	Symbol	Number	Node values
Solar zenith angle (SZA)	θ_0	10	0,30,45,60,70,77,81,84,86,88°
Viewing zenith angle (VZA)	θ	7	0,15,30,45,60,70,75 °
Ozone profile	Ω_p	11	- Low latitude (EQ - 30°N) 225, 275, 325 DU - Mid-latitudes (30°N – 60°N) 225, 275, 325, 375, 425, 475, 525, 575 DU

Surface pressure	P_s	4	1, 0.7, 0.4, 0.25 atm
Wavelength	λ	7	312.34, 317.35, 331.06, 340, 354, 360, 380 nm

Table S2. The variables tabulated in the LUTs of the radiances and Jacobians.

List	Radiance	Jacobian
Zero-order coefficient of I_a	$I_0(\lambda, \theta_0, \theta, \Omega_p, P_s)$	$I'_0(\lambda, \theta_0, \theta, \Omega_p, P_s, Z^*)$
First-order coefficient of I_a	$Z_1(\lambda, \theta_0, \theta, \Omega_p, P_s)$	$Z'_1(\lambda, \theta_0, \theta, \Omega_p, P_s, Z^*)$
Second-order coefficient of I_a	$Z_2(\lambda, \theta_0, \theta, \Omega_p, P_s)$	$Z'_2(\lambda, \theta_0, \theta, \Omega_p, P_s, Z^*)$
Total transmission of the atmosphere	$T(\lambda, \theta_0, \theta, \Omega_p, P_s)$	$T'(\lambda, \theta_0, \theta, \Omega_p, P_s, Z^*)$
Spherical albedo of the atmosphere.	$S_b(\lambda, \Omega_p, P_s)$	$S'_b(\lambda, \Omega_p, P_s, Z^*)$

Z: Partial column ozone at 11 Umkehr layers.

Z*: Z, but where each layer is perturbed by 1DU

50

Lagrange polynomials were used to interpolate the LUTs for the calculated radiance according to the geometry and pressure of each observation. The calculated BUV radiance I_c is subsequently converted to an N-value, as defined in equation (2) of the paper. The Jacobians, which represent the sensitivity of radiance to changes in atmospheric ozone, are a critical input for the Step 2 algorithm. In our algorithm, we compute the Jacobians using a finite difference of radiances (I_c) before and after a small perturbation of 1 DU in the amount of ozone in each layer of the standard ozone profiles in 11 Umkehr layers. Table S2 provides a summary of the variables and dimensions of the Jacobian LUTs.

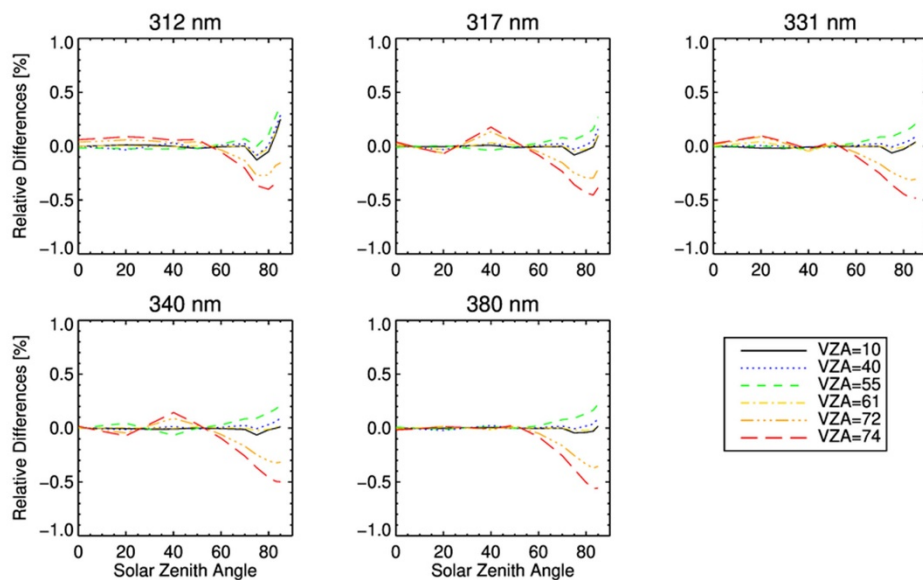
55

S2. Evaluation of radiance interpolation errors

LUT-based simulations of radiances are evaluated against on-line radiative transfer calculation, with the impact of the simulation errors on total column ozone retrievals. Figure S2 shows the relative differences of radiances between LUT simulations and on-line calculations as a function of SZA and VZA for TOMS wavelengths, respectively. The simulation errors are typically less than 0.1 %, except for at extreme SZAs and VZAs. The LUT-based simulations significantly underestimate on-line calculations by up to ~ 0.5% when SZA is larger 60 ° at VZA is larger 70 °. Figure S3 illustrates how

60

65 much these errors contribute on retrieval errors of total column ozone. Our results indicate that LUT errors could cause retrieval errors of up to ~ 3 DU in general.



70 **Figure S2.** Relative differences of of LUT-based radiances to online calculations, as a function of SZA and VZA, for five TOMS wavelengths. Note that the comparison is performed at 12 SZAs (0.1, 10, 20, 30, 40, 50, 60, 70, 75, 80, 83 85 °) and at 12 VZAs (0.1, 10, 20, 30, 40, 50, 55, 58, 61, 67, 72, 74 °).

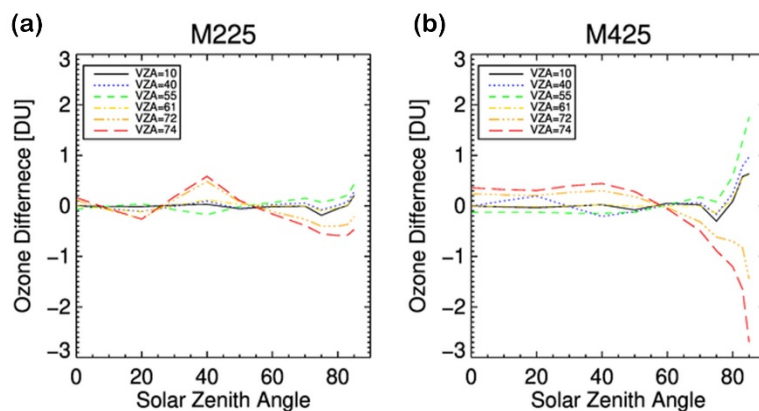


Figure S3. Impacts of LUT-simulation errors on ozone retrieval for (a) low and (b) high column amount cases, respectively.

75 **S3. Information content**

S3.1 GEMS Column Weighting Function

The retrieved total column depends on an a priori profile shape. Column Weighting Functions (CWFs) describes the contribution of either measurement information or a priori information on retrievals at each layer, which is written as:

80

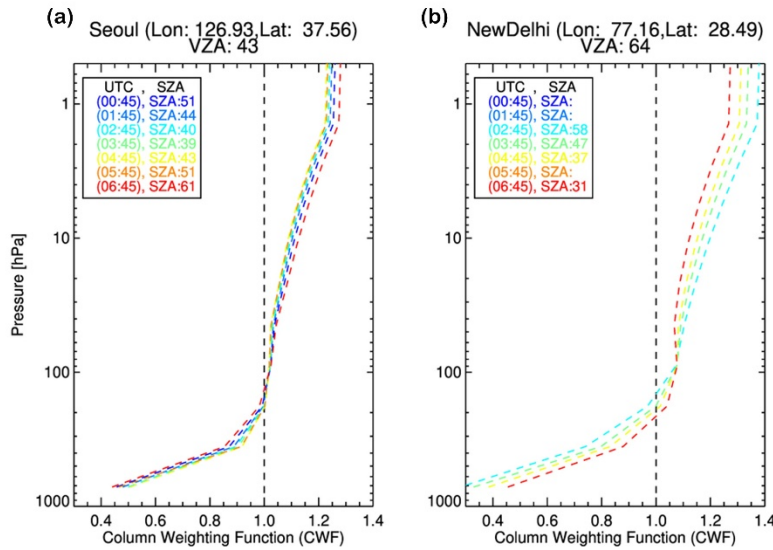
$$CWF(i) = w_i = \sum_{j=1}^{j=11} A(j, i) \quad (S3),$$

where A is the Averaging kernel matrix (Rodgers, 2000). The shape of the CWFs is determined by the sensitivity of the measured radiances to changes in ozone profiles. Figure S4 illustrates the vertical profiles of GEMS CWFs for Seoul and New Delhi on 27 September 2020 under clear sky conditions.

85 CWFs are generally close to 1, indicating high sensitivity to ozone changes in most layers except for the lowest boundary layer where CWFs ranges from 0.0 to 0.7. A value of 1 indicates ideal sensitivity, typically found in the lower stratosphere near 100 hPa, where the greatest variability in ozone profile occurs. Above this level, CWFs values increase beyond 1, indicating oversensitivity to differences between the true ozone profile and a priori, which is likely to add noise and bias to the retrieval.

90 However, since the amount and variation of ozone at these altitudes are small, they generally have little impact on the total column. As shown in Figure S4, CWFs show no significant diurnal variation in Seoul with the mild change of SZAs from 31° at noon and 61° in the late afternoon on September 21, 2020. However, the CWFs in the lower atmosphere decreases as SZA increases, while the CWFs above 100 hPa altitude increases with increasing SZA. This phenomenon is attributed to the change of UV

95 penetration in the atmosphere with increasing SZA, which causes changes in Rayleigh scattering at that altitude. In New Delhi, despite the similar SZA range (31° to 58°) to that in Seoul, the larger observed VZA results in smaller CWFs values in the lower layers and larger CWFs values in the upper layers compared to Seoul.



100

Figure S4. GEMS CWFs for (a) Seoul and (b) New Delhi on 27 September 2020. The VZAs are 43° and 64° at Seoul and New Delhi, respectively. The different colors represent the diurnal variations of CWFs, with the observation time (UTC) and SZAs given in the legend.

105

The contribution of the a priori profile to a total column retrieval can be determined by subtracting the CWFs (\mathcal{W}) from one ($1-\mathcal{W}$). The actual contribution of the a priori profile to a total column retrieval can be determined by multiplying the a priori profile (x_a) by $1-\mathcal{W}$. The vertical distribution of \mathcal{W} and $1-\mathcal{W}$ in Seoul on August 25, 2020 at 08:00, 13:00, and 18:00 KST (shown in Figure S5) illustrates the changes in vertical sensitivity and the influence of a priori on total ozone retrieval with respect to changes in

110

SZA throughout the day. At higher SZA, $1-\mathcal{W}$ exhibits a curve-shaped distribution with large negative values in the lowest layer and negative values at higher altitudes, implying an amplified impact of the a priori profile on ozone retrieval. These findings demonstrate that, in contrast to vertical sensitivity, the impact of the a priori profile is minimal at noon and increases during the late afternoon and early morning due to contrasting sensitivity.

115

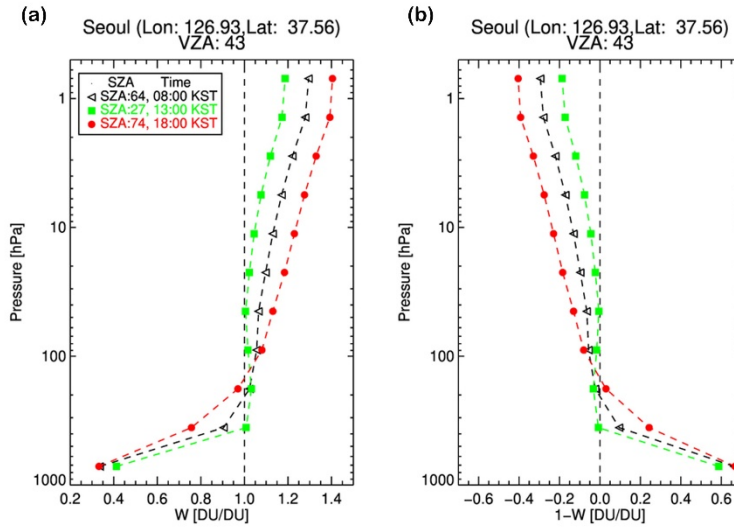


Figure S5. The CWFs (W) (on the left) and $1-W$ (on the right) in Seoul at 0800 (black), 1300 (green) and 1800 (red) KST on 25 August 2020.

120 S3.2 Degree of freedom of the signal (DFS) and error in the retrieved total ozone

The degrees of freedom for signal (DFS) is a useful estimation of the number of independent pieces of information obtained during the retrieval process. It is defined as the sum of the diagonal elements of the averaging kernel matrix according to Rodgers (2000). Since this study uses three wavelengths in the retrieval, the DFS cannot exceed three, with typical values ranging between 1-2.5 depending largely on

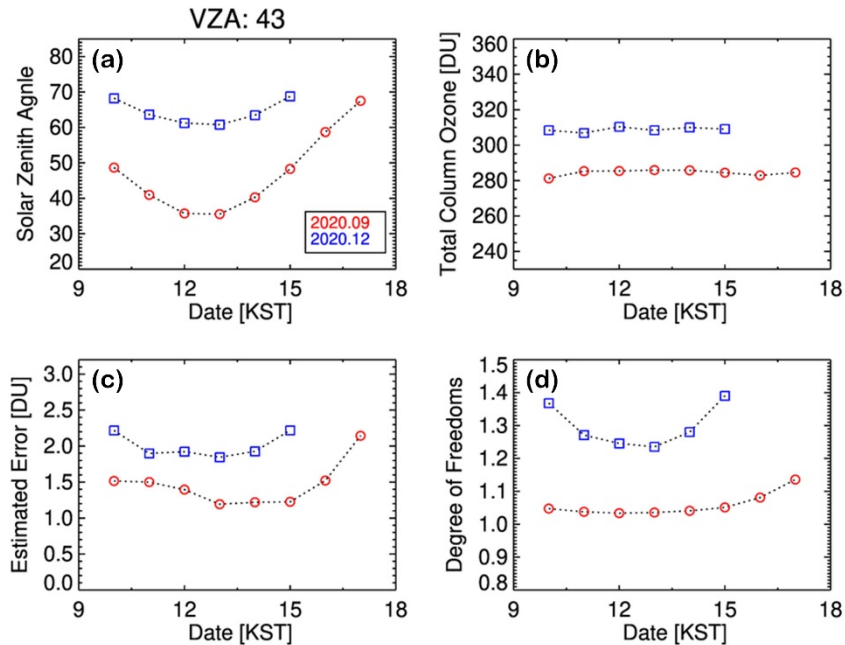
125 viewing geometry. The amount of error (ϵ) in the retrieved total ozone is estimated using equation S4, which means the 1σ uncertainties for the retrieved column.

$$\epsilon = \sqrt{(1 - w_l)S_a(1 - w_l)^T} \quad (\text{S4})$$

Figure S6 shows that the example of the monthly mean values of GEMS SZA, TCO, estimated

130 retrieval errors, and DFS obtained from one-day observations in Seoul for September and December.

Seoul (Lon:126.934,Lat: 37.564), 2020



135 **Figure S6.** The monthly mean values of (a) GEMS SZA, (b) TCO, (c) estimated retrieval errors, and (d) DOFs observed on one-day in Seoul. The red and blue circle symbols in the figure represent observations made in September and December, respectively. The GEMS VZA for these observations at Seoul is 43 °.

140 GEMS observations were conducted eight times in September and six times in December in Seoul. The diurnal variation of SZA in September (35.5 ° to 67 °) is more pronounced than in December (60.8 ° to 68.7 °). The monthly average ozone concentrations in September and December are approximately 280 DU and 310 DU, respectively, with minimal daily variations. Estimated retrieval errors during 145 September range from 1.5 to 2 DU, depending on the variation of SZA, while in December, higher estimated retrieval errors averaging 2 DU are observed only at high SZA. The DFS is almost constant at 1 in September but varies from 1.25 to 1.4 depending on the increase of SZA. These findings indicate some variation in retrieval error and DFS correlated with SZA over the course of a day.